Supplementary Information (SI) for Inorganic Chemistry Frontiers.

Supporting Information

Multidentate chelation via pyridine-based molecules for high-efficiency perovskite solar cells

Yongxiang Zhang[a,b], Jinfeng Zhang[b], Aiqin Sun[b], Zhiqian Yang[b], Mengting Han[b], Yang Huang[b,c], Mei Lyu[a,e], Yan Meng[*d], Jun Zhu[*a] and Linhua Hu[*b]

[a]School of Chemistry and Chemical Engineering Hefei University of Technology Hefei 230009, China

[b]Key Laboratory of Photovoltaic and Energy Conservation Materials, CAS, Institute of Solid State Physics, Hefei Institutes of Physical Science, Chinese Academy of Sciences. Hefei, Anhui, 230031, China

[c]Anhui Institute of lnnovation for Industrial Technology, Hefei, Anhui 230088, China

[d]Department of Physics, Xingtai University, Xingtai, Hebei, 054001, China

[e]Postdoctoral Workstation, AnHui SunWay Cable Co., Ltd., No. 18, Gaoxin Avenue, Gaogou Industrial District, Wuwei, 238339, China

[*]Corresponding author.

E-mail address: 200221007@xttx.edu.cn; lhhu@rntek.cas.cn; jzhu@hfut.edu.cn

Experimental Section

Materials

CsCl (99.99%), chlorobenzene (CB 99.9%), tin (II) chloride ($SnCl_2$, reagent grade, 98%), 4-tert-Butylpyridine (tBP), bis(trifluoromethane)sulfonimide lithium salt, tris(2-(1H-pyrazol-1-yl)-4-4 tertbutylpyridine) cobalt (III) (FK209) and HCl (4 M in 1,4-dioxane) were obtained from Sigma-Aldrich. PbI_2 (99.99%), imide iodide (FAI), methylammonium iodide (MAI), methylammonium chloride (MACl), *spiro*-OMeTAD (99.8%) and poly-(3,4-ethylenedioxythiophene)-poly (styrene sulfonic acid ester) (PEDOT: PSS, 1.3-1.7wt% solution in water) were obtained from Xi'an Polymer Light Technology Corp. Dimethyl sulfoxide (DMSO, 99.9%), Dimethylformamide (DMF) were obtained from J&K. diethyl 2,6-Pyridinedicarboxylate (DIP) and isopropyl alcohol (IPA) were purchased from Aladdin. All the chemicals were utilized in the form they were obtained, with no additional purification processes applied.

Device fabrication

Photovoltaic devices are fabricated using the structure of glass/FTO /SnO_2/perovskite/DIP/*spiro*-OMeTAD/Au. The patterned FTO substrate (15 Ω per square) was sequentially cleaned using acetone, isopropanol and deionized water for 15 min by means of ultrasonic cleaning.

A 2 M $SnCl_2$ stock solution in ethanol was first prepared by dissolving $SnCl_2$ in ethanol and then stored in the refrigerator at 5 °C. The FTO substrate was soaked in a dilute $SnCl_2$ solution (1:50 molar ratio of 2 M aqueous $SnCl_2$ stock solution and cold deionized water) in a glass container. Then the glass container was placed in a drying cabinet at 70 °C for 3 h. After cooling down, the FTO substrate was rinsed with ethanol and deionized water three times. Finally, the substrate was annealed on a hotplate at 180 °C for 1 h. These substrates are treated with UVO one more time for 20 min after cooling down to room temperature. After the UVO treatment, the perovskite solution (1.4 M, prepared by mixing presynthesized FAI, MAI, MACl powder, CsCl and PbI_2 powder in cosolvent of DMF and DMSO at a volume ratio of 7: 3) is spin-coated on the treated FTO substrates at 1000 rpm for 10 s and 5000 rpm for 35 s. Chlorobenzene (100 μL) as anti-solvent is slowly dropped on the surface of the rotating substrate at the 25th second during the spin-coating process. The perovskite-covered substrate is annealed at 100 °C for 50 min in air glove box and 150 °C for 10 min in air at the humidity of 20-30%. The interface layer is formed on the perovskite film by spin-coating 50 μL of DIP solution (dissolve it in IPA) at 5000 rpm for 25 s. The *spiro*-

OMeTAD layer is spin-coated from a solution of 72.3 mg of *spiro*-OMeTAD, 28.8 μL of tBP, and 17.5 μL of Li-TFSI solution (520 mg Li-TFSI in 1 mL ACN) in 1 mL of anhydrous chlorobenzene at 4000 rpm for 30 s. All the above processes are completed in the air glove box. Finally, the Au electrode is deposited using a thermal evaporator under ca. 1.0×10^{-4} Torr for 60 nm at the rate of 0.2 Å/s.

Device characterizations

The X-ray diffraction (XRD) analysis was conducted utilizing a 9 kW Rigaku Smart Lab X-ray diffractometer, equipped with Cu-Kα radiation at a wavelength of 1.540593 Å, scanning over an angular range from 5° to 65° (2θ). The scanning electron microscopy (SEM) and elemental analysis were executed by a high-resolution field-emission scanning electron microscope (FE-SEM, Sirion 200, FEI Corp., Holland). The ultraviolet-visible (UV-Vis) and transmittance spectra were acquired from TU-1901 spectrophotometer (PGENERAL, Beijing) and U-3900H spectrophotometer (HITACHI, Japan). Fourier transform infrared spectrometer (FTIR, iS50R, America) was applied to characterize the structure. The X-ray photoelectron spectroscopy (XPS) measurements were performed on a Thermo Fisher Scientific ESCALAB250XI. The liquid-state 1H NMR spectra were measured by a nuclear magnetic resonance spectrometer (BRUKER AV400). The Kelvin probe-force microscopy (KPFM) images were captured using the NT-AIST equipment in Peak Force KPFM mode. The QM400-TM system, equipped with a 450 nm laser excitation source, was used to document the steady-state photoluminescence (PL) measurements. The photoluminescence (PL) mappings were measured by LabRAM HR Evolution (excitation wavelength: 473nm). KPFM was performed by Veeco MultiMode V. Time-resolved photoluminescence (TRPL) spectra were captured through the application of the Time-Correlated Single Photo Counting (TCSPC) technique, with excitation supplied by a 450 nm wavelength picosecond diode laser from Edinburgh FS1000. The perovskite films on glass/FTO were examined at standard room temperature for all associated measurements. Utilizing an electrochemical workstation (Autolab 302N, Metrohm, Switzerland), Electrochemical impedance spectroscopy (EIS) measurements were taken within a frequency span of 1 Hz to 1 MHz in a dark enclosure, applying a 10 mV AC modulation. The obtained impedance spectra were fitted with Nova software (v2.1.4, Metrohm, Switzerland). The *J*–*V* characteristics of the photovoltaic device were acquired by a Keithley 2420 source meter under an irradiation intensity of 100 mW cm^{-2}, employing an Air Mass 1.5 Global (AM 1.5 G) solar simulator (0.0739 cm^2 active area). The monochromatic incident photon-to-electron conversion efficiency (IPCE) spectra were collected from 300 to 900 nm by Newport QE Kit (PV Measurements, Inc.).

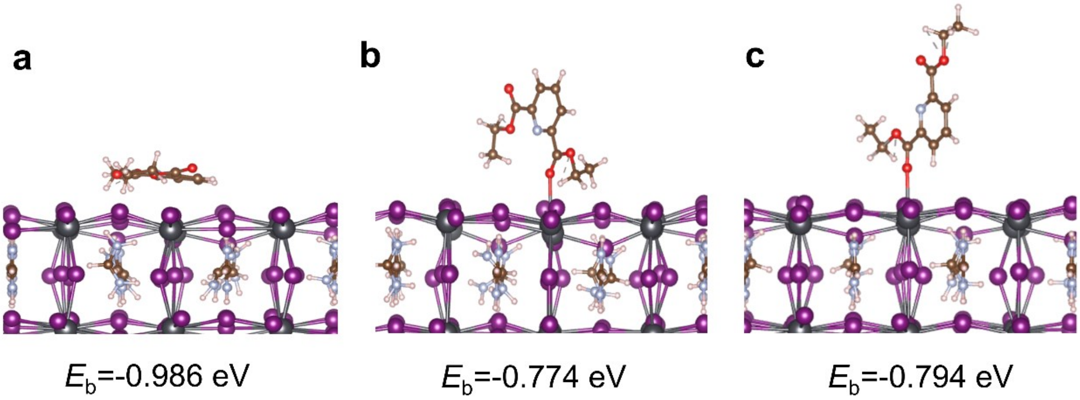

Figure S1. DFT modeling of the binding energy of DIP molecules with different configurations on Perovskite surface.

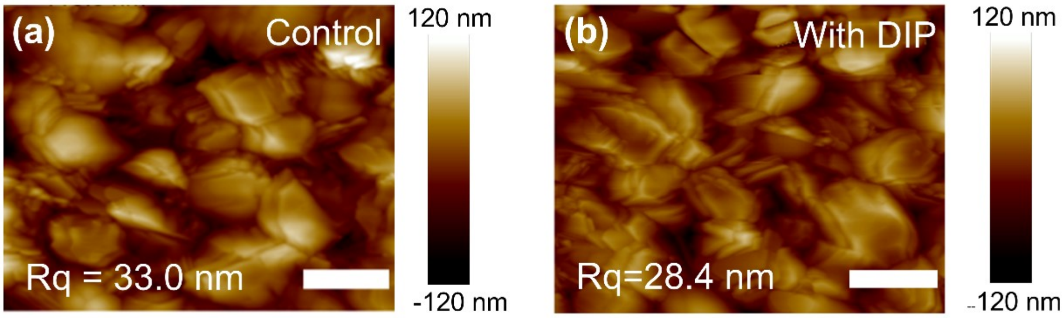

Figure S2. AFM images of the pristine perovskite and DIP-treated perovskite films (scale bar, 1μm).

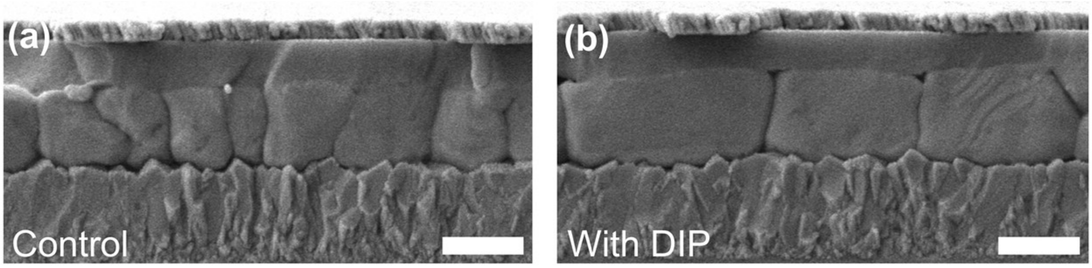

Figure S3. Cross-sectional SEM images of pristine perovskite and DIP-treated perovskite films (scale bar, 0.5μm).

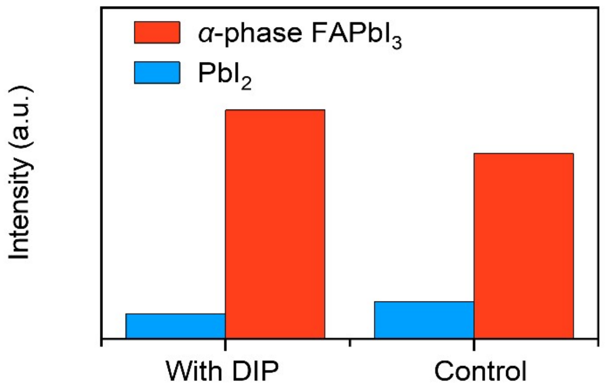

Figure S4. The ratio of *α*-phase $FAPbI_3$ peak intensity to PbI_2 peak intensity.

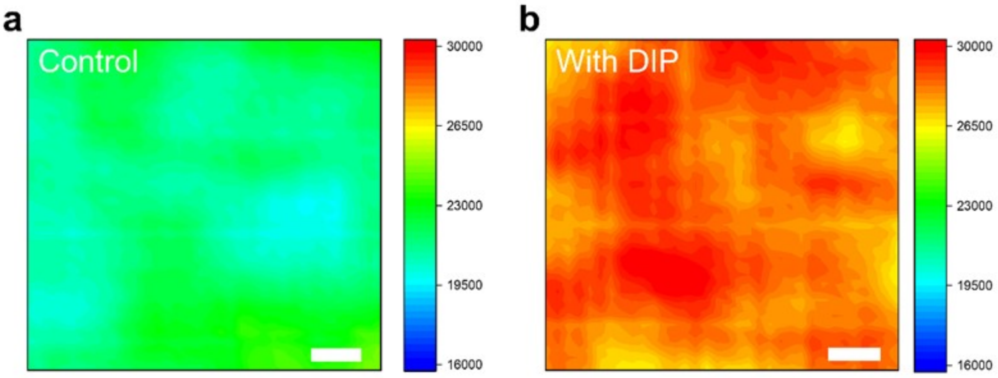

Figure S5. PL mappings of perovskite films on FTO, Control and with DIP (scale bar, 2 μm).

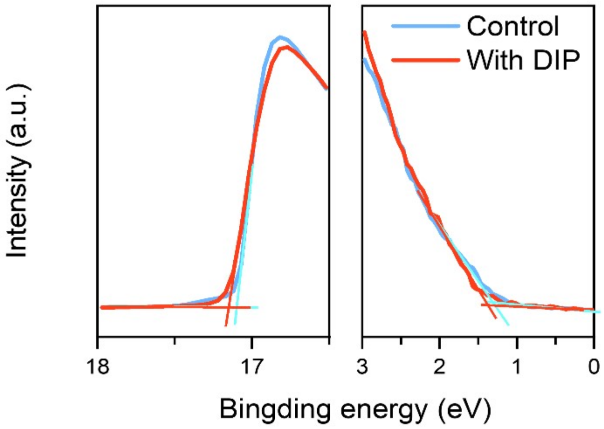

Figure S6. UPS spectra of secondary electron cutoff region and valence band region of perovskite films without and with DIP.

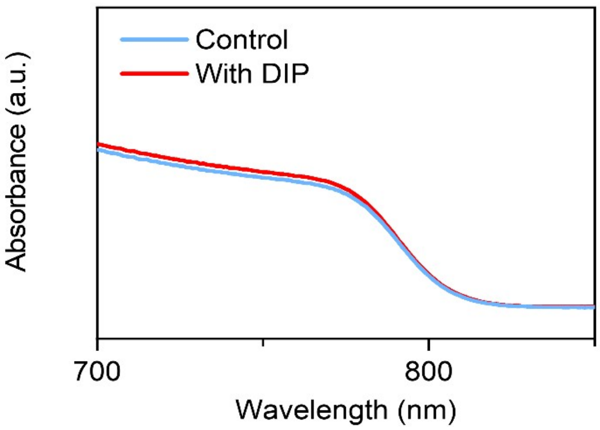

Figure S7. UV-Vis absorption spectra of perovskite films without and with DIP.

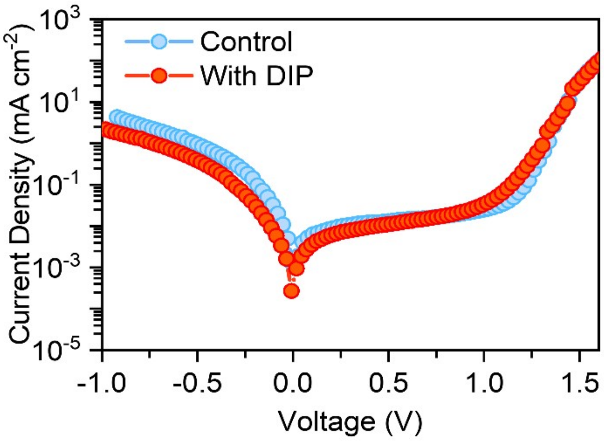

Figure S8. Dark current of the PSCs without and with DIP modification.

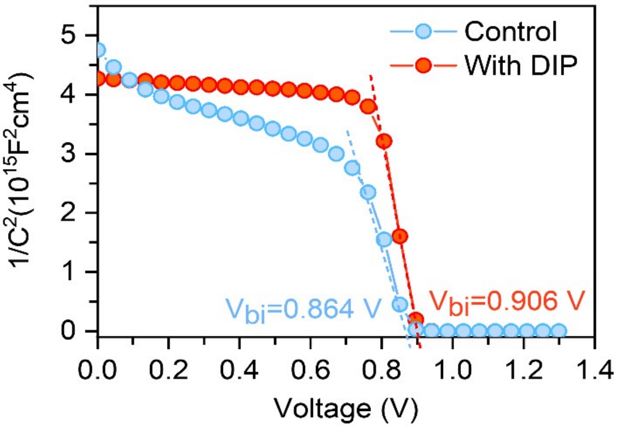

Figure S9. Mott-Schottky plots of the PSCs without and with DIP.

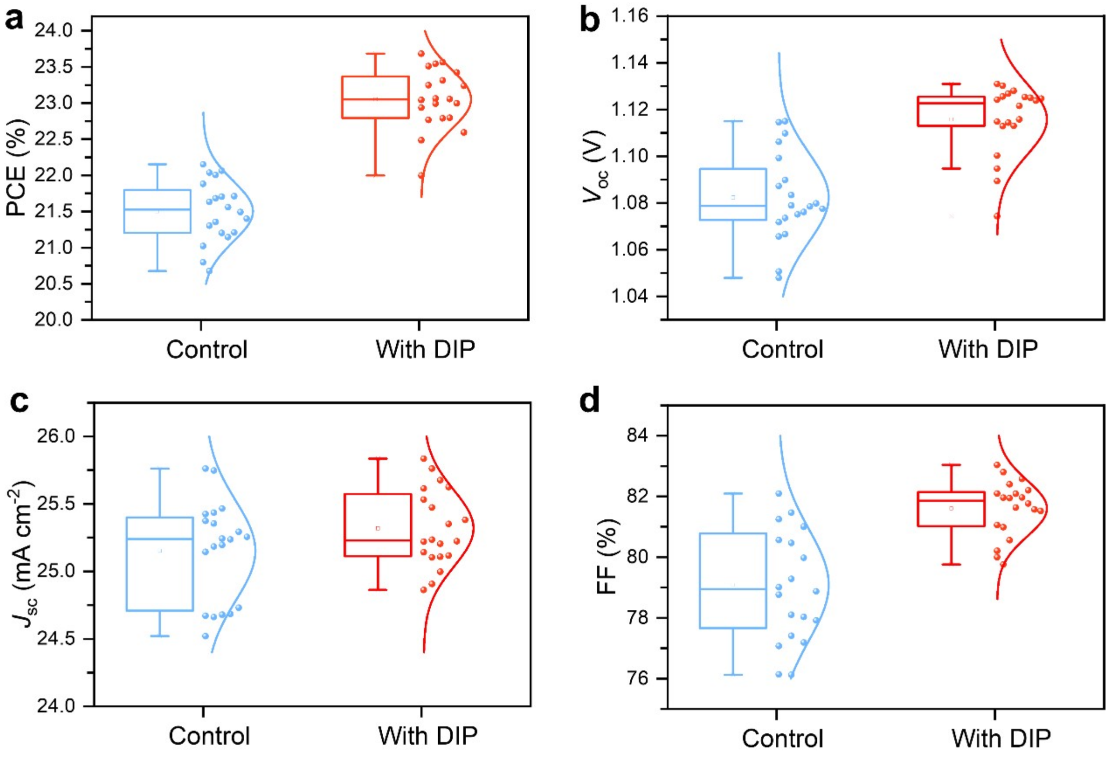

Figure S10. Photovoltaic parameters statistics of (a) PCE, (b) V_{oc}, (c) J_{sc}, and (d) FF based on 20 devices with or without DIP modification.

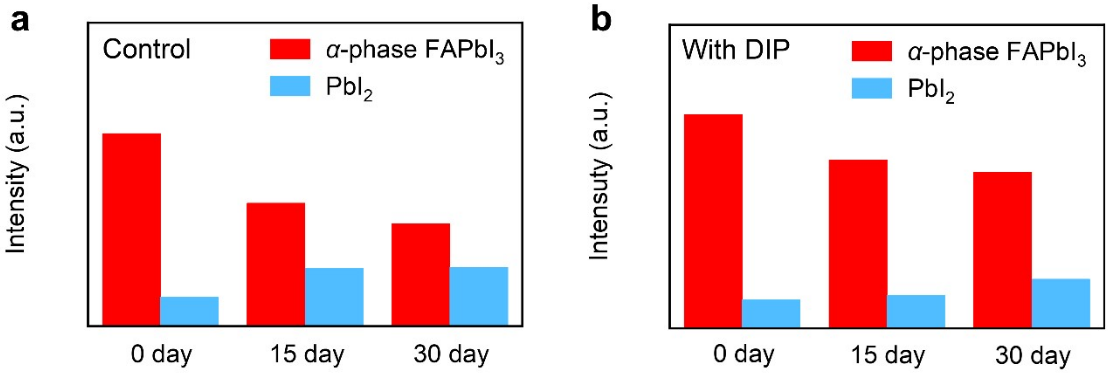

Figure S11. The ratio of α-phase $FAPbI_3$ peak intensity to PbI_2 peak intensity at the humidity of 65 ± 5% after 30 days. For control device, the ratio of α-phase $FAPbI_3$ peak intensity to PbI_2 peak intensity are 6.42, 2.11, 1.73 after 0 day, 15 days, 30 days. For DIP-modified device, the ratio of α-phase $FAPbI_3$ peak intensity to PbI_2 peak intensity are 7.39, 5.10, 3.16 after 0 day, 15days, 30 days.

Table S1. TR-PL parameters of the perovskite or SnO_2/perovskite films with or without DIP modification.

Sample	**τ_1 (ns)**	**τ_2 (ns)**	**A_1**	**A_2**	**τ_{ave} (ns)**
Glass/perovskite	42.89	232.07	2384.67	504.05	143.82
Glass/perovskite/DIP	172.15	1004.53	1549.22	577.93	739.83

Table S2. Parameters for the control and the DIP-modified devices.

Sample	**Scan directions**	**V_{oc} (V)**	**J_{sc} (mA cm^{-2})**	**FF (%)**	**PCE (%)**
Control	Forward	1.10	25.42	78.76	22.15
	Reverse	1.06	25.32	75.09	20.31
1 mg/mL DIP	Forward	1.12	25.01	80.48	22.63
	Reverse	1.09	25.05	77.74	21.31
2 mg/ml DIP	Forward	1.10	25.32	82.60	23.10
	Reverse	1.08	25.44	78.57	21.60
3 mg/ml DIP	Forward	1.13	25.83	81.05	23.68
	Reverse	1.11	25.90	78.88	22.82
4 mg/ml DIP	Forward	1.11	25.75	80.67	23.09
	Reverse	1.09	25.55	77.06	21.48
5 mg/ml DIP	Forward	1.09	25.12	82.36	22.75
	Reverse	1.06	25.41	75.35	20.32